THE JOURNAL OF PHYSICAL CHEMISTRY B

ARTICLE

pubs.acs.org/JPCB

Effect of Molecular Weight on the Adsorption Characteristics of Lignosulfonates

Yonghong Deng,[†] Weijian Zhang,[†] Yuan Wu,[†] Haifeng Yu,[‡] and Xueqing Qiu*,[†]

[†]State Key Lab of Pulp and Paper Engineering, School of Chemistry and Chemical Engineering, South China University of Technology, Guangzhou, 510640, People's Republic of China

[‡]Top Runner Incubation Center for Academia-Industry Fusion, and Department of Materials Science and Technology, Nagaoka University of Technology, 1603-1 Kamitomioka, Nagaoka 940-2188, Japan

ABSTRACT:

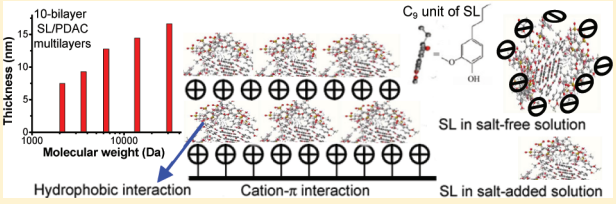

Sequentially adsorbed multilayers composed of sodium lignosulfonate (SL) and poly(diallyldimethylammonium chloride) (PDAC) were built up by a layer-by-layer self-assembly technique to investigate the adsorption characteristics of SL microgels for sensitivity improvement. The effect of molecular weight on the adsorption characteristics was investigated by light scattering, UV−visible spectroscopy, ellipsometer, X-ray photoelectron spectroscopy (XPS), atomic force microscopy (AFM), and contact angle measurements. Results show that the self-assembly of SL microgels and PDAC is not mainly driven by electrostatic interaction but by cation−π interaction and hydrophobic interaction. The Coulomb interaction in SL microgels causes a "slow mode" peak in dynamic light scattering measurement, but it can be completely suppressed when SL is dissolved in 1.2 mol/L NaCl solutions due to charge-screening. The SL in 1.2 mol/L NaCl solutions can be well adsorbed on a PDAC surface, indicating that the electrostatic interaction is not the main driving force. The presence of cation−π interaction between SL and PDAC is detected by a stoichiometric ratio of SL to PDAC in SL/PDAC self-assembled films. During SL/PDAC self-assembly, hydrophobic interaction plays an important role in determining the adsorption rate, film thickness, surface morphology, and surface properties. SL with a higher M_w has a stronger hydrophobic ability in water, so it exhibits a slower adsorption rate, a larger film thickness, and a higher film roughness. SL with different M_w has almost the same wettability because of a larger hydrophobic effect that increases contact angle and a higher film roughness that decreases contact angle. In this case, the opposite effects cancel each other to make no difference in wettability, but it still reflects the role of the hydrophobic effect in surface properties.

INTRODUCTION

As the second most abundant renewable resource in plants, lignin has attracted worldwide attention because of the growing crises of oil resources and environmental pollution.[1,2] Other than as a component of wood, sodium lignosulfonate (SL) is mostly presented as a byproduct in spent liquor from the paper and pulping industry. Because of favorable wettability, adsorptivity, and dispersive ability, SL can be used as an anionic surfactant in various application areas.[3−6] When SL is used as a dispersant, some groups of SL act as an anchor to be adsorbed on the solid surfaces, and the other groups are exposed to water. SL enhances the stability of solid suspension in water because of steric hindrance and the electrostatic repulsive force. The application of SL in the field of anionic surfactants depends on the adsorption characteristics of SL on solid particles. Until now, how to utilize lignin with high efficiency has been a great challenge. A better understanding of the adsorption characteristics of lignosulfonates is required to improve its value-added application.

As an anionic surfactants, the performance of lignosulfonates is significantly affected by molecular weight.[7−11] Qiu et al. found that lignosulfonates with different molecular weight have different adsorption behaviors and dispersion ability when used as a dispersant for pesticide and water−coal-slurry.[7−9] Ansari and Pawlik investigated the adsorption behaviors of lignosulfonates on chalcopyrite and molybdenite, and discovered that lignosulfonates with higher molecular weight fractions tended to preferentially adsorb over lower molecular weight components.[10] Anderson et al. considered that lignosulfonates with higher molecular weight show a higher dispersion stability.[11] Although the adsorption phenomena of SL on the dispersed solid particles have been widely reported,[7−11] the adsorption characteristics of lignosulfonates at solid−liquid interfaces are unclear, and the effect of molecular weight on the adsorption characteristics is not fully understood.

Received: August 28, 2011
Revised: October 22, 2011
Published: November 01, 2011

How to understand the adsorption characteristics of a SL layer at a molecular level has become a worldwide difficult problem. First, the raw SL material recovered from the spent pulping liquor has a wide molecular weight distribution and unknown salt content, and the molecular conformation of SL in solutions is a very complex microgel.[12,13] The current adsorption theory about polymers or small molecules cannot explain the adsorption behaviors of SL. Second, existing industrial applications of SL indicate that the dispersed solid particles are of all kinds of shapes, but the adsorbed thickness of lignosulfonate is very thin,[13,14] which makes it hard to determine the microstructure of the SL layer adsorbed on the solid particles. For example, atomic force microscopy (AFM) images of the surface cannot echo the real morphology of an SL layer, but rather a mixed image of the SL layer together with the substrate. UV−visisible (UV−vis) spectroscopy cannot be used to monitor the adsorption process because the absorbance at a characteristic wavelength is too weak to be detected perceptibly. To overcome the first difficulty, the raw SL is required to be purified carefully, and an SL sample with a narrow molecular weight distribution and known salt content is necessary for fundamental investigation. To overcome the second difficulty, we can select smooth surface substrates instead of irregular solid particles, and build up layer-by-layer (LBL) self-assembled multilayers instead of a thin SL monolayer. LBL self-assembly, which was first noted by Iler,[15] and then rediscovered by Decher and Hong,[16] is a simple and controllable technique of depositing multilayers by the consecutive adsorption of alternating anionic and cationic species, and the newly created film surface is mostly dependent on the chosen polyelectrolytes and adsorption conditions.[17] Therefore, LBL self-assembly technique is considered to be a useful method for investigating the adsorption characteristics of SL, as it can be well characterized by a wide variety of physical techniques.

In the current work, five SL fractions with low polydispersity index were carefully prepared by gel column chromatography separation, and then were used as a polyanion to fabricate LBL self-assembled multilayers on smooth quartz slides. The adsorption kinetics of SL during the self-assembly of multilayers was monitored by UV−vis spectroscopy, and the thickness of SL/PDAC multilayers was measured by an ellipsometer. AFM was used to observe the surface morphology, and X-ray photoelectron spectroscopy (XPS) measurement was used to characterize the ratio of SL to PDAC during the self-assembly process. During self-assembly, the adsorption characteristics of SL film, such as the driving force, the adsorbed amount, the adsorption rate, surface morphology, and wettability, were carefully analyzed in terms of molecular weight.

EXPERIMENTAL METHODS

Materials. The raw SL, supplied by Shixian Papermaking Co. Ltd. (China), was recovered from spent sulfite pulping liquor. SL aqueous solutions (10 wt %) were first filtered to remove the insoluble solid matter, and then the low M_w impurities were removed by using an ultrafiltration apparatus (Wuxi Membrane Science and Technology Co., China) with a 1000 Da (Da) cutoff membrane. Five SL fractions with narrow M_w distribution were obtained through the method of gel column chromatographic separation.[18] Since ionic strength and solution pH have a great influence on the solution behaviors and the adsorption characteristics, salt-free SL samples with constant solution pH are required for the fundamental investigation of the effect of molecular weight on the adsorption characteristics. To remove salt, SL separated by column chromatography was further treated by column chromatography with water as an eluant, and then followed by dialysis against water. The solution pH of SL samples was about 6.7 after dialysis, and was then kept unchanged for sample preparation.

Poly(diallyldimethylammonium chloride) (PDAC, M_w of 200 000−350 000, 20% solution, Aldrich) was used as a polycation and was diluted to a concentration of 0.1 mmol/L (repeated unit). Water used in this work was ultrapure water obtained from a Millipore water purification system, and the water resistivity was larger than 18 MΩ·cm. The other reagents were purchased commercially as analytical-grade products and used directly without further purification unless otherwise indicated.

Characterization. The M_w and distributions of SL were determined by gel permeation chromatography (GPC) with Ultrahydragel 120 and Ultrahydragel 250 columns. The 0.10 mol/L $NaNO_3$ aqueous solution with pH 8 was used as the eluent at a flow rate of 0.5 mL/min. The effluent was monitored at 280 nm with a Waters 2487 UV Absorbance Detector (Waters Corp., USA) at a flow rate of 1.0 mL/min. Poly(styrene sulfonate) (PSS) was employed as the standard substance.

Elemental analysis of SL was performed by an Elemental Analyzer (PE-2400 II, Perkin-Elmer). The contents of the sulfonic groups of SL were measured according to the methods described in ref 19.

The UV−vis absorption measurements were performed with a UV−vis spectrophotometer (UV-2450, Shimadzu Corp., Japan). For the sample solutions with water as the solvent, water was scanned at the same wavelength as a baseline.

Dynamic light scattering (DLS) was performed on a commercial light scattering instrument (ALV/CGS-3, Germany) equipped with a multi-τ digital time correlator (ALV-7004) and a solid−state He−Ne laser (JDS-Uniphase, output power = 22 mW, at = 632.8 nm). The effect of fluorescent emission on the light−scattering of SL was eliminated by inserting a high performance laser-line bandpass filter (NT47-494) between the sample solution and the detector unit.[20,21] The absorption of SL in the investigated concentration range is very weak at a incident laser wavelength of 632.8 nm, so the effect of absorption on the light scattering is neglected.

Film thickness was determined by a spectroscopic ellipsometer (UVISEL-NIR-FGMS, Horiba). Surface morphology and surface roughness was measured by AFM (DI Multimode SPM nanoscope V, Veeco). The ratio of SL to PDAC in the SL/PDAC films was studied using XPS by a Krato Axis Ultra DLD spectrometer with AL K_α X-ray ($h\nu$ = 1486.8 eV) at 15 kV and 150 W. The advanced contact angle of the SL/PDAC film was measured using a DCAT21 tensiometer (Dataphysics Company, Germany).

Self-Assembled Film. The SL/PDAC LBL self-assembled films of desired bilayers were deposited on smooth quartz slide substrates (50 × 14 × 8 mm). Prior to deposition, the quartz slide was sonicated in a 98% H_2SO_4/30%H_2O_2 solution (piranha solution) for 1 h and in a $H_2O/H_2O_2/NH_4OH$ (5:1:1) solution for 1 h followed with a thorough rinse and dried with an air stream. A freshly treated quartz slide was first kept dipped into the polycation solution for about 10 min. The slide was thoroughly rinsed with ultrapure water and blown dry with air. The slide was then dipped into the polyanion solution for an equal amount of time and extensively rinsed with the same solvent as the polyanion solution and blown dry. This process was repeated

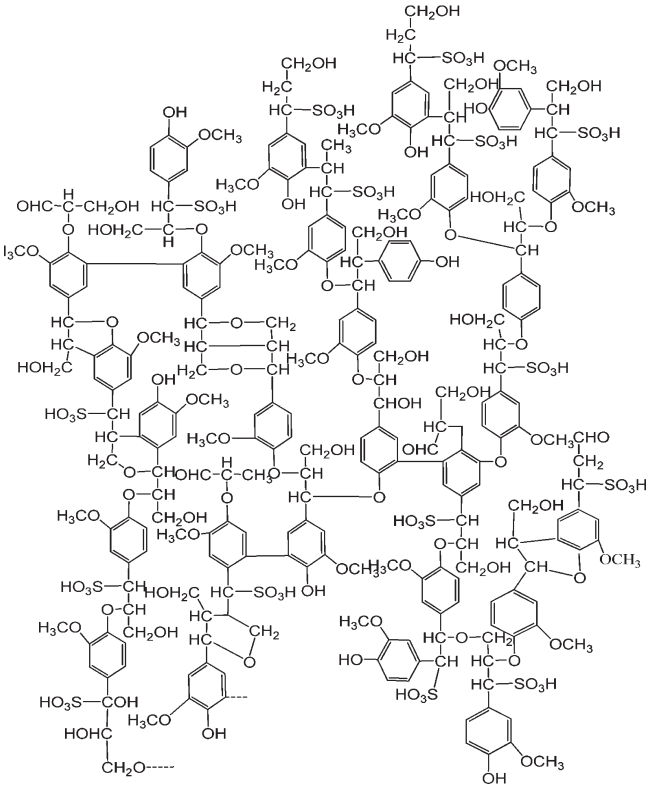

Figure 1. Proposed chemical structure of lignosulfonic acid.

until multilayers with the required number of layers were achieved.

For the investigation of adsorption kinetics of SL, a 10-bilayer SL/PDAC multilayer with PDAC as the outermost layer was used as a substrate for the self-assembly of SL and PDAC. This substrate was dipped into the SL solutions for the required time, and then rinsed with water for 1 min and blown dry for UV−vis measurement. This process was repeated until the saturated adsorbed amount of a SL layer was reached.

RESULTS AND DISCUSSION

The structure of SL is very complex (Figure 1). It consists of phenyl-propanoid units (C_9 unit), sulfonic groups, and other functional groups. The raw SL was carefully purified by filtration, ultrafiltration, chromatographic separation, and dialysis. After being treated by dialysis against the ultrapure water, the SL samples were considered "salt-free" samples. SL fractions with narrow M_w distribution were prepared by gel column chromatographic separation for the following fundamental investigation.[18] Figure 2 shows the M_w distributions of SL and its five fractions prepared by column choromatography. Before chromatographic separation, SL had a weight-averaged M_w of 10 500 Da with a polydispersity index larger than 4.5. After chromatographic separation, each of the five SL fractions had a separated M_w with a low polydispersity index. Besides M_w distribution, SL also has polydispersity in the loading density of the sulfonic groups. The loading density of the sulfonic groups decreases at elevated molecular weight (Table 1). In the present work, we studied the solution behaviors and the adsorption characteristics of SL with narrow molecular weight distribution and known ionic strength. The details will be given in the following parts.

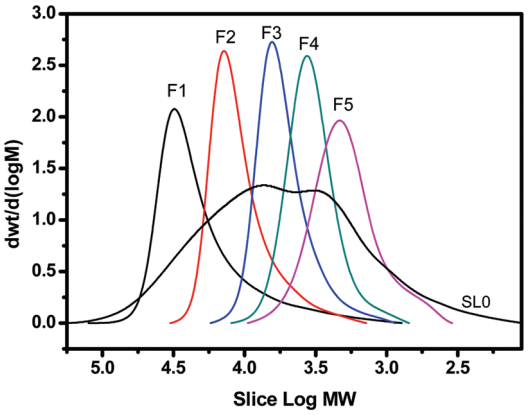

Figure 2. Weight-average molecular weight distributions of SL (before separation) and its five fractions after gel column chromatographic separation.

Table 1. Molecular Weight, Polydispersity, and Sulfonic Content of the SL Fractions

SL samples	M_w (g/mol) (by GPC)	polydispersity	sulfonic groups/ SL (mol/g)
F1	31127	1.21	1.052×10^{-3}
F2	13937	1.17	1.127×10^{-3}
F3	6392	1.15	1.148×10^{-3}
F4	3625	1.20	1.316×10^{-3}
F5	2133	1.36	1.616×10^{-3}

Diffusion Coefficient of SL in Solutions. DLS was used to determine the diffusion coefficient (D) of SL in aqueous solutions. Figure 3 shows the DLS results of 0.8 g/L SL (F3) in 0.1 mol/L NaCl solutions by a CONTIN analysis, measured at different angles. SL exhibits a bimodal decay rate distribution corresponding to a "fast mode" and "slow mode". The origin of the "fast mode" is attributed to the translational self-diffusion of the single molecules,[22] and that of the "slow mode" may be related to the Coulomb interactions in polyelectrolytes.[23,24]

Coulomb interactions can be eliminated by adding enough salt into charged polymers, and then the decay rate peak for the "slow mode" was depressed.[23,24] As shown in Figure 4, when salt is added into the SL (F3) solutions gradually, the decay rate peak for the "fast mode" does not change much, but the decay rate peak for the "slow mode" decreases gradually with increasing NaCl concentration, and finally disappears when the NaCl concentration reaches 1.2 mol/L. The results support the suggestion that the "slow mode" is related to the coulomb interactions in polyelectrolytes.[23,24] According to Förster et al., Coulomb interactions become negligible if the molar concentration ratio $c_{monomer}/c_{salt} < 25$ for branched charged polymers (or $c_{monomer}/c_{salt} < 1$ for linear charged polymers);[23,24] therefore, the theoretical NaCl concentration to eliminate the Coulomb interactions of SL was calculated to be about 4×10^{-5} mol/L for branched structure (or 9.0×10^{-4} mol/L for linear structure). However, the actual salt content required to eliminate the Coulomb interactions of SL is much larger than the theoretical salt content. The reason for this phenomenon is unclear. The possible explanation is that the structure of SL consists of compact microgels,[12,13] and the penetration of the hydrated

counterions inside the polyelectrolyte body should be more difficult in a compact microgel than in a branched or linear charged polymer.[25]

Figure 5a shows the DLS results of 0.8 g/L SL (F3) in 1.2 mol/L NaCl solutions by a CONTIN analysis, measured at different angles. SL exhibits a monomodel decay rate distribution corresponding to the "fast mode", and the "slow mode" shown in Figure 3 was completely depressed.[22−24] The diffusion coefficients of the "fast mode" (D_f) were calculated to be 5.92×10^{-7} cm^2/s from the slope of the decay rate versus q^2 (Figure 5b). On the basis of the diffusion coefficient D, the hydrodynamic radius R_h of F3 can be estimated to be 4.1 nm according to the Stokes−Einstein relation.[22] Here, SL itself is not necessarily a sphere, and the R_h is the radius of an equivalent sphere that has a diffusion coefficient D identical to that of the SL particle during its Brownian motion in solution.

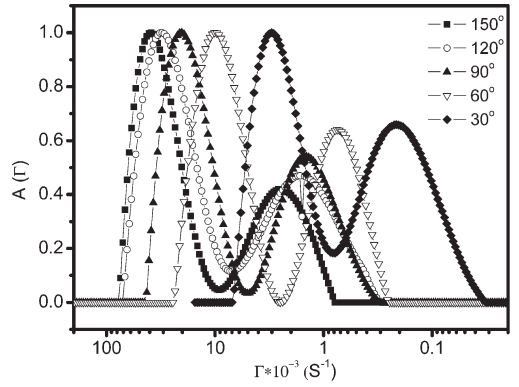

Figure 3. CONTIN analysis of 0.8 g/L SL solution in 0.1 mol/L NaCl solutions, measured by DLS at different detector angles. Here, the SL sample is F3.

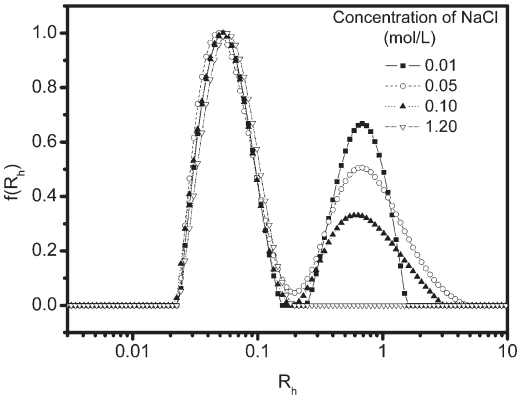

Figure 4. CONTIN analysis of 0.8 g/L SL (F3) with different salt concentrations, measured at a detector angle of 90°, where the "fast" mode has little change, but the "slow" mode is suppressed with increasing salt concentration.

Table 2 shows the diffusion coefficient (D) and hydrodynamic radius (R_h) of five SL fractions in 1.2 mol/L NaCl solutions. With increasing molecular weight, the diffusion coefficient D decreases and the corresponding R_h increases, indicating that the molecular size of a single SL increases.

SL/PDAC Self-Assembled Multilayers. SL fractions with narrow M_w distribution and known salt content were used as polyanion to build up self-assembled multilayers with PDAC as an oppositely charged polyelectrolyte. UV−vis absorption spectroscopy was used to monitor the self-assembly process of SL/PDAC multilayer films. It was found that salt-free SL could hardly adsorb on PDAC. This failure in adsorption is related to the specific microgel structure of SL in aqueous solutions, which is different from linear or branched polyions that can form well-defined self-assembled multilayers.[17,26] However, SL dissolved in a 1.2 mol/L NaCl solution was well adsorbed on PDAC to form SL/PDAC multilayers. Figure 6 gives the UV−vis spectra of the SL/PDAC multilayer films obtained from SL (F1) in 1.2 mol/L NaCl solution, varying with the number of bilayers. The λ_{280nm} is considered to be the characteristic absorption peak of SL. Except for the first three bilayers having a substrate effect, a linear increase of the absorbance with the increase of the number of bilayers is observed, which indicates that the deposition process is reproducible from layer to layer.

Table 2. Diffusion Coefficient (D) and Hydrodynamic Radius (R_h) of Five SL Fractions in 1.2 mol/L NaCl Solutions

SL samples	D (cm^2S^{1-})	R_h (nm)
F1	3.03×10^{-7}	8.1
F2	4.14×10^{-7}	5.9
F3	5.92×10^{-7}	4.1
F4	1.02×10^{-6}	2.4
F5	1.31×10^{-6}	1.9

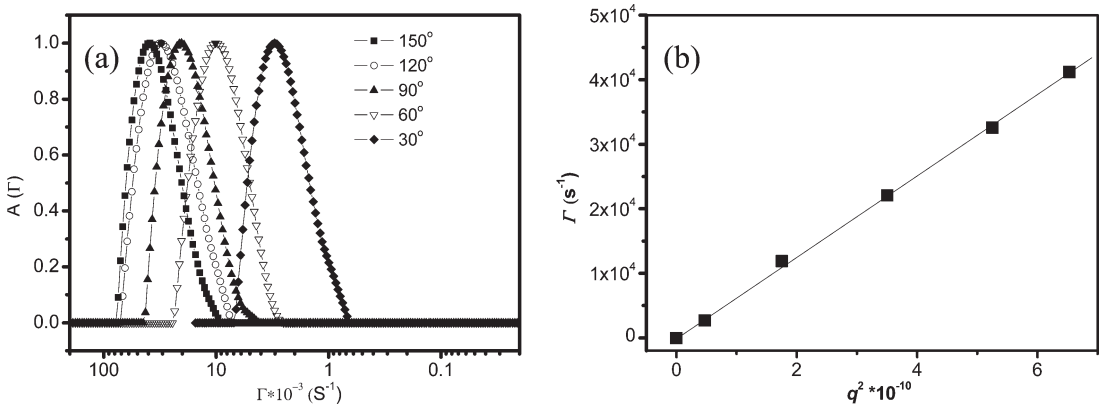

Figure 5. (a) CONTIN analysis of 0.8 g/L SL (F3) in 1.2 mol/L NaCl solution, measured by DLS at different detector angles. (b) Variation of the decay rate as a function of q^2.

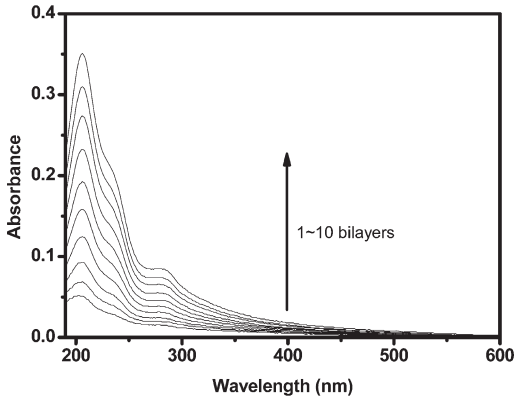

Figure 6. UV−vis spectra of SL/PDAC multilayers with different bilayer numbers, where the SL sample is 0.1 wt % F1 dissolved in 1.2 mol/L NaCl solution at pH 6.7.

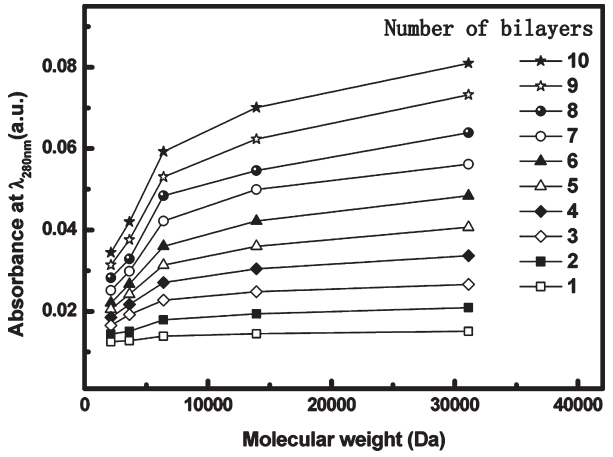

Figure 7. Relationship of Molecular weight of SL and the absorbance of SL/PDAC multilayers at λ_{280nm} (0.1 wt % SL, 1.2 mol/L NaCl, pH = 6.7).

The adsorption behaviors contributed by each SL layer depends on molecular weight. Figure 7 shows the absorbance at $\lambda_{280\ nm}$ of the SL/PDAC multilayers as a function of the molecular weight. The absorbance value of SL contributed by each SL layer has an obvious increase with increasing molecular weight.

The film thickness of the SL/PDAC multilayers was measured by optical ellipsometry. Figure 8 shows the film thickness of the 10-bilayer SL/PDAC multilayers versus molecular weight. For comparison, the effect of molecular weight on the absorbance at λ_{280nm} is also presented in Figure 8. The relationship between the absorbance values and M_w is similar to that between the film thickness and M_w, which indicates that the adsorbed amount of SL during the self-assembly process can be well monitored by UV−vis absorption spectroscopy. The SL with higher M_w has a larger film thickness; therefore, lignosulfonates with higher M_w show a better dispersion ability[10,11] because of a larger steric hindrance and a stronger electrostatic repulsive force.

The film thickness of SL/PDAC self-assembled film increases with increasing M_w (Figure 8), but the values of the thickness are much smaller than the hydrodynamic radii of the SL singular molecule (Table 2). This phenomenon can be explained in this

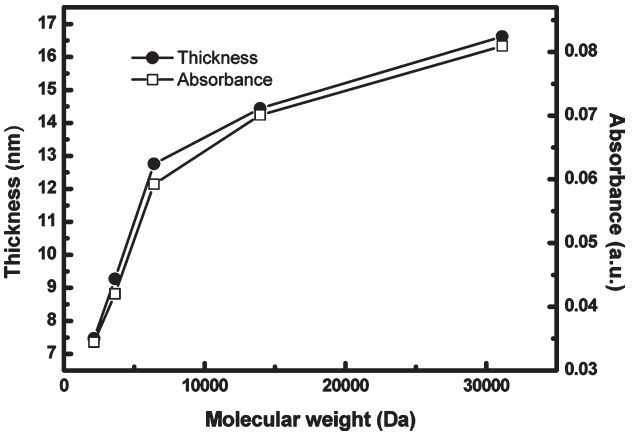

Figure 8. The absorbance and thickness of 10-bilayer SL/PDAC multilayers, which are obtained from SLs (0.1 wt % SL, 1.2 mol/L NaCl, pH = 6.7) with different molecular weights.

way. SL has a flat microgel structure, with one dimension much smaller than the other two,[13,14] so SL may be adsorbed on PDAC with the smallest dimension perpendicular to the film surface, resulting in a film thickness much less than the hydrodynamic radius.

Adsorption Mechanism. Electrostatic interaction is widely accepted for the LBL self-assembly mechanism.[17,26] However, hydrophobic interaction, hydrogen bonding, and other short-range van der Waals interactions, may also play a role during the LBL self-assembly, and in some cases, can determine whether stable multilayers form.[27] For the adsorption mechanism of lignin-based polyanions on PDAC, there exist three opinions: Notley and Norgren considered the driving force of PDAC on alkali lignin during the self-assembly process as pure electrosorption in nature;[28] Paterno and Mattoso investigated the effect of pH on the preparation of self-assembled films of poly(*o*-ethoxyaniline) and sulfonated lignin, and concluded that the adsorption at higher pHs was related to the hydrogen bonding interactions.[29] Pillai and Renneckar suggested that there exists cation−π interaction between lignin and PDAC.[30]

In our case, the salt-free SL has a strong electrostatic interaction with PDAC, but it can hardly adsorb on the PDAC surface because of SL's specific microgel structure. When enough salt (e.g., 1.2 mol/L NaCl) is added into the SL solutions, the charged groups of SL are completely screened (Figure 4), but the adsorption amount of SL is large (Figure 7). Obviously, the electrostatic interaction is not the main driving force for the self-assembly of SL and PDAC, but the hydrophobic interaction plays an important role during the self-assembly process.

Since urea is a hydrogen-bonding blocking reagent, the addition of urea into SL is supposed to detect the effect of hydrogen bonding on the SL/PDAC self-assembly. Figure 9 shows the absorbance at 280 nm of the SL/PDAC multilayers, prepared from SL with or without urea. To avoid the pH effect, the solution pHs of SL with and without urea were adjusted to be 6.7. As shown in Figure 9, the absorbed amount of SL during SL/PDAC self-assembly has no obvious change when the hydrogen-bonding blocking reagent urea is added into it, indicating that hydrogen bonding interactions do not play an important role in the adsorption of SL on PDAC. This phenomenon may be caused by two reasons: one is that PDAC is neither an acceptor nor a donor of hydrogen bonding; the other is that the addition of

urea has no obvious effect on the molecular configuration and the aggregation behaviors of SL in water.

The ratio of SL to PDAC in the self-assembled film was examined by XPS, which was expected to give a clue for the existence of cation−π interaction between PDAC and SL. As shown in Figure 8, the 10-bilyer SL/PDAC multilayers are about 7−17 nm, so the averaged thickness of an SL/PDAC bilayer is about 0.7−1.7 nm. The XPS is normally used to provide elemental composition of the surface of typically the top 1−10 nm. This detection depth is about the same or larger than the SL/PDAC self-assembled bilayer; therefore, it is suitable to analyze the elemental composition of SL and PDAC in the SL/PDAC self-assembled film. Table 3 shows the elemental analysis of the SL/PDAC films by XPS, where element S represents the sulfonic content of SL, and element N represents the PDAC content. The S/N ratio in the SL/PDAC films decreases with increasing molecular weight. The ratio of SL to PDAC in the films was calculated based on the sulfonic content of each SL fraction and the S/N ratio in films. As shown in Table 3, the ratio of SL to PDAC in the five SL/PDAC films is almost the same if taking experimental error into account, indicating that there exists a stoichiometric ratio of SL to PDAC because of the presence of a cation−π interaction between SL and PDAC.

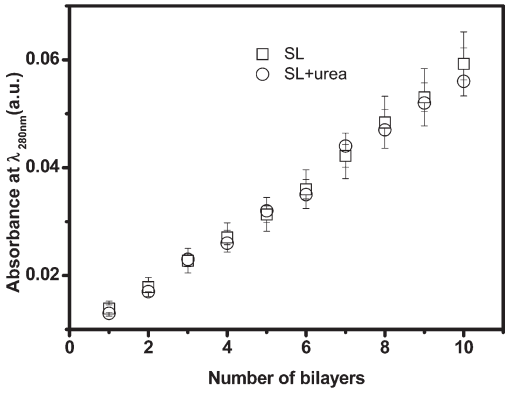

Figure 9. UV−vis spectra of SL/PDAC multilayers with different bilayer numbers, where the SL sample is 0.1 wt % F3 dissolved in 1.2 mol/L NaCl solution at pH 6.7. Urea is added into SL solution to detect the effect of hydrogen bonding on the SL/PDAC self-assembly.

Figure 10 gives an illustration for the adsorption behaviors of SL on PDAC. The salt-free SL can hardly be adsorbed on the PDAC surface, but SL in salt-added solution can be well adsorbed on PDAC, indicating that the electrostatic interaction is not the main driving force for the self-assembly of SL and PDAC. The self-assembly of SL and PDAC may be mainly driven by the cation−π interaction between SL and PDAC, and the hydrophobic interaction really plays an important role in the SL adsorbed amount. As shown in the histograms of Figure 10, the SL with higher M_w has a larger hydrophobic ability, resulting in a larger film thickness.

Adsorption Kinetics of SL during Self-Assembly. Since the first several bilayers have a substrate effect, a 10-bilayer SL/PDAC multilayer with PDAC as the outermost layer was used as the substrate for investigating the adsorption kinetics of SL. Figure 11 shows the adsorption kinetics curves of the five SL fractions. The absorbance at 280 nm of a SL layer varies with the adsorption time, and each measurement contains a drying step. The adsorption of a SL layer reaches saturation within a few minutes. The kinetics curves of absorbance (A) versus time (t) can be fitted by second-order exponential decay (eq 1), and the parameters calculated by fitting the data are recorded in Table 4.

$$A = A_0 + k_1 \exp(-t/\tau_1) + k_2 \exp(-t/\tau_2) \quad (1)$$

where k_1, and k_2 are constants, and τ_1 and τ_2 are the characteristic times. A_0 is the absorbance at equilibrium; that is to say, the absorbance grows gradually with increasing time and then reaches a saturation value. The saturated absorbance is A_0, taken as proportional to the adsorbed amount of SL.

Table 3. Elemental Analysis of the SL/PDAC Films by XPS

SL samples	sulfonic groups/SL (mol/g)	N (mol)	S (mol)	S/N (mol/mol)	[a]SL/PDAC (g/mol)
F1	1.052×10^{-3}	2.218	1.992	0.898	854
F2	1.127×10^{-3}	1.517	1.475	0.972	863
F3	1.148×10^{-3}	2.396	2.395	1.000	871
F4	1.316×10^{-3}	1.815	2.084	1.148	872
F5	1.616×10^{-3}	1.505	2.126	1.413	874

[a] SL/PDAC = (S/N)/(sulfonic groups/SL).

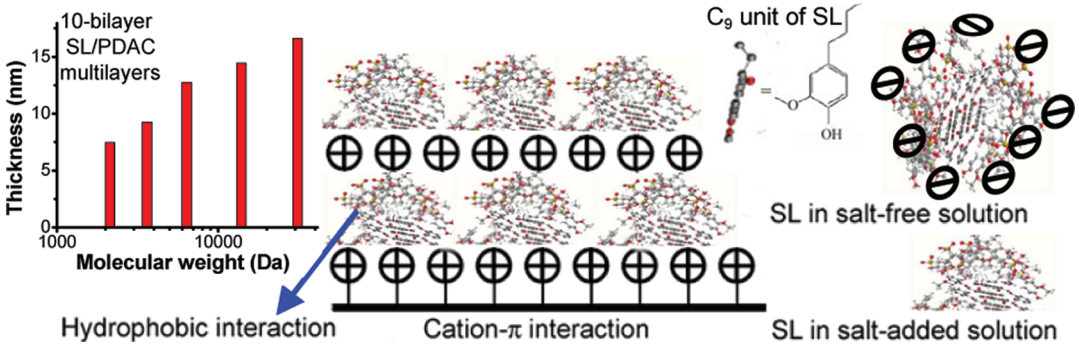

Figure 10. Schematic representation for the adsorption behaviors of SL in saline solutions.

dx.doi.org/10.1021/jp208312a |J. Phys. Chem. B 2011, 115, 14866–14873

Obviously, there exists a two-step process of adsorption during the self-assembly of SL/PDAC. The initial stage of adsorption is related to the polymer molecules being transferred from the dipping solution to the solid surface, while the second stage corresponds to the rearrangement of polymer molecules on the solid surface.[31] As shown in Table 4, the characteristic times (τ_1 and τ_2) increase with increasing molecular weight. The adsorption rate is the reciprocal of the characteristic time, so the adsorption rate decreases with increasing molecular weight. A slower adsorption rate at higher molecular weight is caused by lower diffusion coefficient (D), as shown in Table 2. Table 4 also shows that the saturated adsorbed amount of an SL layer increased with increasing molecular weight. Compared with the regular LBL adsorption process (Figure 7), the saturated adsorbed amount of a SL layer containing several drying interferences showed a larger increase, resulting from the competitive adsorption between water and SL.[31]

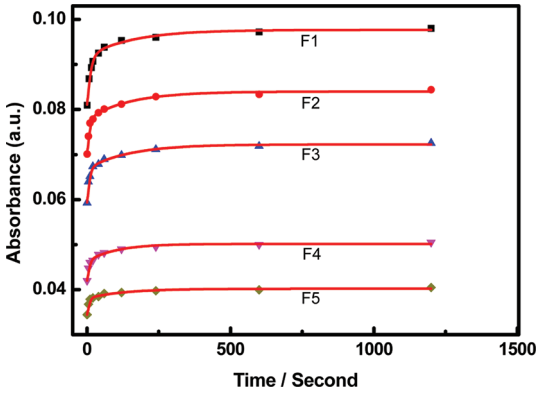

Figure 11. Absorbance at $\lambda_{280\ nm}$ versus immersion time for adsorption of a SL layer on the already formed 10-bilayer SL/PDAC multilayers. The SL layer was obtained from SLs (0.1 wt % SL, 1.2 mol/L NaCl, pH = 6.7) with different molecular weights.

Table 4. Adsorption Parameters Used for Fitting the Experimental Data of Kinetics Curves of SL During Self-assembly

SL samples	A_0	k_1	τ_1 (s)	k_2	τ_2 (s)	R^2
F1	0.0977	−0.1073	10.85	−0.0059	159.58	0.9933
F2	0.0840	−0.0078	6.61	−0.0062	146.61	0.9910
F3	0.0722	−0.0075	6.34	−0.0055	145.82	0.9913
F4	0.0502	−0.0029	5.38	−0.0052	130.77	0.9845
F5	0.0402	−0.0023	4.94	−0.0060	128.40	0.9908

Surface Property of the SL/PDAC Self-Assembled Films. AFM is a powerful tool to identify surface morphology and microstructure characteristics. Figure 12 shows the AFM topographic images of the SL/PDAC multilayers obtained from five SL fractions with SL as the outmost layer. Obviously, SL with a lower molecular weight has a smoother surface. The root-mean-square (rms) roughness of the SL layer can be calculated from the topographic image, and it increases with molecular weight; namely, F1: 2.09 nm, F2: 2.04 nm, F3: 1.41 nm, F4:0.83 nm, F5: 0.78 nm.

The surface wettability of the SL/PDAC multilayers can be detected by measuring the contact angle. The smaller the contact angle, the more wettable the surface. Figure 13 shows the contact angle of SL/PDAC multilayers prepared from five SL fractions with SL as the outmost layer. The contact angle does not change much with the molecular weight, and all the contact angles of the five SL/PDAC multilayers are about 60°. This phenomenon can be explained this way. On one side, SL with higher molecular weight has a stronger hydro-

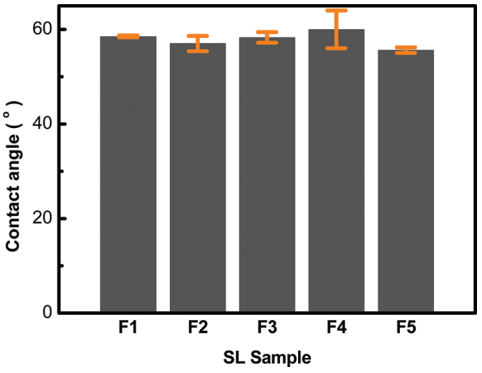

Figure 13. Advancing contact angle of 10-bilayer SL/PDAC self-assembled multilayers with SL as the outmost layer. The SL layer was obtained from SL (0.1 wt % SL, 1.2 mol/L NaCl, pH = 6.7) dipping solutions with different molecular weights.

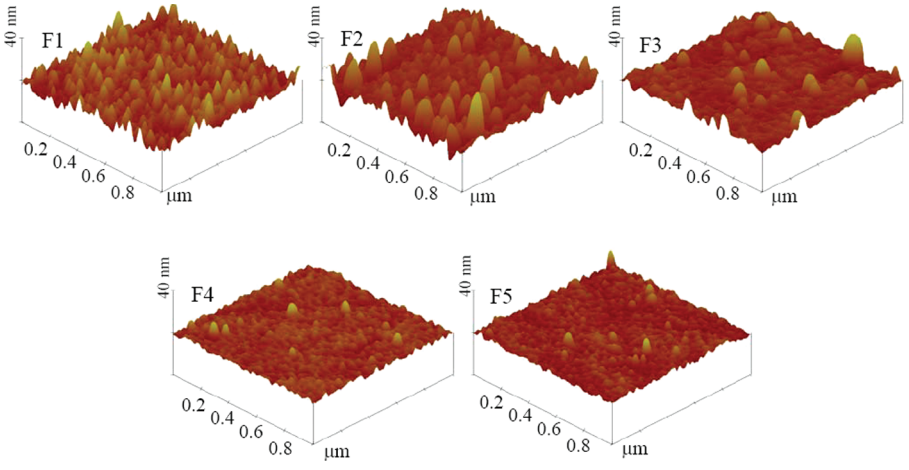

Figure 12. AFM images of the 10-bilayer SL/PDAC self-assembled multilayers with SL as the outmost layer. The SL layer was obtained from five SL fractions (0.1 wt % SL, 1.2 mol/L NaCl, pH = 6.7).

dx.doi.org/10.1021/jp208312a |J. Phys. Chem. B 2011, 115, 14866–14873

phobic interaction, resulting in a larger contact angle. On the other side, the surface roughness increases with molecular weight. For the same hydrophilic surfaces, a larger roughness results in a smaller contact angle.[32] Because of the two opposite effects, the surface wettability of the SL/PDAC multilayers obtained from SL with different molecular weight is almost the same.

CONCLUSIONS

Five SL fractions with low polydispersity index were carefully prepared by gel column chromatography separation, and then were used as a polyanion to fabricate LBL self-assembled multilayers with PDAC on smooth quartz slides for investigating the effect of molecular weight on the adsorption characteristics of SL microgels. Results show that the self-assembly of SL microgels and PDAC is not mainly driven by electrostatic interaction but by cation$-\pi$ interaction and hydrophobic interaction. DLS measurement of SL shows a bimodal decay rate distribution corresponding to a "fast mode" and "slow mode". The origin of the "fast mode" peak is attributed to the translational self-diffusion of the single molecules, and that of the "slow mode" peak is related to the Coulomb interaction in polyelectrolytes. When SL is dissolved into 1.2 mol/L NaCl solutions, the Coulomb interaction is eliminated, and the "slow mode" peak is completely suppressed. In 1.2 mol/L NaCl solutions, the charged groups of SL were screened, but SL can still be well adsorbed on the PDAC surface, indicating that electrostatic interaction is not the main driving force, but hydrophobic interaction plays an important role during self-assembly. The presence of cation$-\pi$ interaction between SL and PDAC is proved by a stoichiometric ratio of SL to PDAC in SL/PDAC self-assembled films. Because of hydrophobic interaction, the adsorbed amount and surface roughness increase with increasing molecular weights. For five SL fractions, the averaged film thickness of SL is much smaller than the hydrodynamic radius of SL single molecules in solutions, suggesting that SL may have a flat microgel structure, and SL may be adsorbed on PDAC with the smallest dimension perpendicular to film surface. The diffusion coefficient D of SL in 1.2 mol/L NaCl solutions decreases with increasing molecular weight, and the corresponding adsorption rate decreases. The dynamic contact angle indicates that there is no obvious difference in wettability for the five SL/PDAC films due to the two opposite interactions. On one hand, SL with higher molecular weight has a stronger hydrophobic effect that increases the contact angle. On the other hand, SL with higher molecular weight induces a higher film roughness that decreases the contact angle. The studies above offer a useful method for better understanding the effect of molecular weight on the adsorption characteristics of SL microgels at the molecular level for the first time, which is helpful for further expanding the functionalities of SL through manipulation of the adsorption capacity by changing molecular weight.

AUTHOR INFORMATION

Corresponding Author

*Tel.: 86−20−87114722. Fax: 86−20−87114721. E-mail: xueqingqiu66@163.com.

ACKNOWLEDGMENT

The authors acknowledge the financial support of the China Excellent Young Scientist Fund (20925622), the National Natural Science Foundation of China (20976064, 21006036), and Science and Technology Projects of Guangdong Province of China (2009B050600004).

REFERENCES

(1) Lora, J. H.; Glasser, W. J. *J. Polym. Environ.* **2002**, *10*, 39.
(2) Deng, Y. H; Feng, X. J.; Zhou, M. S.; Qian, Y.; Qiu, X. Q. *Biomacromolecules* **2011**, *12*, 1116.
(3) Ouyang, X. P.; Ke, L. X.; Qiu, X. Q.; Guo, Y. X.; Pang, Y. X. *J. Dispersion Sci. Technol.* **2009**, *30*, 1.
(4) Zhou, M. S.; Qiu, X. Q.; Yang, D. J.; Lou, H. M.; Ouyang, X. P. *Fuel Process. Technol.* **2007**, *88*, 375.
(5) Li, Z. L.; Pang, Y. X.; Lou, H. M.; Qiu, X. Q. *Bioresources* **2009**, *4*, 589.
(6) Ouyang, X. P.; Qiu, X. Q.; Lou, H. M.; Yang, D. J. *Ind. Eng. Chem. Res.* **2006**, *45*, 5716.
(7) Li, X. N.; Qiu, X. Q.; Lou, H. M.; Ouyang, X. P.; Pang, Y. X. *Fine Chem.* **2009**, *26*, 755.
(8) Yang, D. J.; Qiu, X. Q.; Zhou, M. S.; Lou, H. M. *Energy Convers. Manage.* **2007**, *48*, 2433.
(9) Zhou, M. S.; Qiu, X. Q.; Yang, D. J.; Lou, H. M. *J. Dispersion Sci. Technol.* **2006**, *27*, 851.
(10) Anita, A.; Marek, P. *Miner. Eng.* **2007**, *20*, 600.
(11) Anderson, P. J.; Roy, D. M.; Gaidis, J. M. *Cem. Concr. Res.* **1988**, *18*, 980.
(12) Rezanowich, A.; Goring, D. A. J. *J. Colloid Sci.* **1960**, *15*, 452.
(13) Goring, D. A. I.; Vuong, R.; Gancet, C.; Chanzy, H. *J. Appl. Polym. Sci.* **1979**, *24*, 931.
(14) Palmqvist, L.; Holmberg, K. *Langmuir* **2008**, *24*, 9989.
(15) Iler, R. K. *J. Colloid Interface Sci.* **1966**, *21*, 569.
(16) Decher, G.; Hong, J. D. *Makromol. Chem. Macromol. Symp.* **1991**, *46*, 321.
(17) Decher, G. *Science* **1997**, *277*, 1232.
(18) Ouyang, X. P.; Zhang, P.; Tan, C. M.; Deng, Y. H.; Yang, D. J.; Qiu, X. Q. *Chin. Chem. Lett.* **2010**, *21*, 1479.
(19) Lin, S. Y.; Dence, C. W. *Methods in Lignin Chemistry*; Springer-Verlag: Berlin, 1992.
(20) Stacey, K. A. *Light-Scattering in Physical Chemistry*; Academic Press: New York, 1956.
(21) Contreras, S.; Gaspar, A. R.; Guerra, A.; Lucia, L. A.; Argyropoulos, D. S. *Biomacromolecules* **2008**, *9*, 3362.
(22) Schärtl, W. *Light Scattering from Polymer Solutions and Nanoparticle Dispersions*; Springer: Berlin, 2007.
(23) Förster, S.; Schmidt, M. *Adv. Polym. Sci.* **1995**, *120*, 51.
(24) Förster, S.; Hermsdorf, N.; Böttcher, C.; Lindner, P. *Macromolecules* **2002**, *35*, 4096.
(25) Mafé, S.; Manzanares, J. A.; Kontturi, A. K.; Kontturi, K. *Bioelectrochem. Bioenerg.* **1995**, *38*, 367.
(26) Zhang, H. Y.; Yan, X. J.; Wang, Y. W.; Deng, Y. H; Wang, X. G. *Polymer* **2008**, *49*, 5504.
(27) Hammond, P. T. *Curr. Opin. Colloid Interface Sci.* **2000**, *4*, 430.
(28) Notley, S. M; Norgren, M. *Biomacromolecules* **2008**, *9*, 2081.
(29) Paterno, L. G.; Mattoso, L. H. C. *Polymer* **2001**, *42*, 5239.
(30) Pillai, K. V.; Renneckar, S. *Biomacromolecules* **2009**, *10*, 798.
(31) Raposo, M.; Pontes, R. S.; Mattoso, L. H. C.; Oliveira, O. N. *Macromolecules* **1997**, *30*, 6095.
(32) Chen, W.; Fadeev, A. Y.; Hsieh, M. C.; Öner, D.; Youngblood, J.; McCarthy, T. J. *Langmuir* **1999**, *15*, 3395.